

Star Clusters, Planets, Asteroids and Comets in the Light of Big Data

Maria Sizova¹, Sergei Vereshchagin¹, Aleksandr Tutukov¹, and Andrei Fionov²

¹ Institute of Astronomy, Russian Academy of Sciences, Pyatnitskaya str., 48, 119017
Moscow, Russia sizova@inasan.ru

² OCRV (Russian Railway), Triumphalnaya 1, Sochi, 354340 Russia
fionovs@mail.ru

Abstract. Planetary (exoplanetary) systems can lose comets, asteroids, and planets due to their host stars close approaches. Such encounters may occur during stars motion in the Galaxy disk. In this work, we calculate the number of pairwise encounters of the stars inside the open star cluster Hyades and in the selected volume of field stars in order to estimate the number of interstellar small bodies in the Galaxy. The resulting catalog was compiled with data obtained by the *Gaia* spacecraft. *Gaia* data amount is increasing and systematically updating. These factors are fit into the Big Data concept.

Keywords: Open star clusters · Solar System · Planets · Exoplanets · Comets · Big Data

1 Introduction

Recent researches of seemingly completely different phenomena, such as an increasing number of exoplanets (for example, see [2]), rogue planets [9], exocomets [10], interstellar comets [4] and the evolution of open star clusters (OSC) [17] allowed a new look at the scale of the exchange of matter between celestial bodies and systems. To estimate the scales of the phenomena, it is necessary to make calculations based on available Big Data. In addition, the calculations become statistically significant only when there are conclusions based on a large amount of data.

If the star has a planetary system, thus, it has asteroids, comets, and planets (ACP). In the paper [22], based on the analysis of the distribution of binary stars by angular momentum, it was shown that nearly 30% of stars have planetary systems. Modern observational data obtained with the Kepler spacecraft [11] do not contradict this estimate.

The interstellar ACP may occur when stars approach each other. The first idea to calculate the influence of close passages of stars on the Oort cloud comets was proposed by [20]. The author showed that the effect of changing the speed of comets in the Oort cloud of the Sun becomes significant at approaches distances less than 1 pc. Nowadays, using modern *Gaia* spacecraft data, the investigation of the close encounters of the field stars with the Solar system and resulting

Copyright © 2021 for this paper by its authors. Use permitted under Creative Commons License Attribution 4.0 International (CC BY 4.0).

effect on the Oort cloud comets is carrying out by many authors (for example, see [21], [3]).

Purpose. We aim to estimate the volume of the population of small interstellar bodies in the Galaxy generated by paired stellar encounters of the field stars and encounters within OSCs. Then, we integrate stellar orbits backward up to 500 Myr, and calculate the close approaches of a limited sample of stars, then extrapolate the obtained data to the Galaxy.

Data and Methods. We use the last available release of the *Gaia* spacecraft catalog [6], which is currently best suited for the implementation of our task. To integrate the stellar orbits, we use *galpy* [5] for *python* programming language.

Structure. In section 2 we explain how we proceed data and show our first results of the calculations (pairwise encounters of the stars samples), section 3 explains the main result of our calculations (close approaches up to 1 pc) and makes some predictions about the number of the ACP in the Galaxy. Work summarizing presented in section 4.

2 *Gaia* Data Description

In order to statistically estimate the star paired approaches frequency in the Galaxy disk and find stars that had close encounters up to 1 pc, we used the most precise available data from *Gaia Early Data Release 3 (Gaia EDR3 [7])*. We aim to compare interstellar ACP production by selected volume of the field stars and OSC, hence we chosen the most studied open cluster Hyades.

Our task is to choose *Gaia EDR3* stars for which is available data allowing us to integrate the orbits in their motion around the Galactic Center. Thus, we load data and filter stars with available positions on the sky (right ascension and declination α, δ), proper motions (μ_α, μ_δ), parallaxes (π) and radial velocities (V_r).

Data Quality and Quantity. The full astrometric *Gaia* solution (5 parameters) – $\alpha, \delta, \mu_\alpha, \mu_\delta, \pi$ – for around 1.468 billion sources, with a limiting magnitude of about $G \sim 21$ (mag hereinafter) and a bright limit of about $G \sim 3$ (for more details, see [1]).

The parallax uncertainties are

- 0.02 – 0.03 mas for $G < 15$
- 0.07 mas at $G = 17$
- 0.5 mas at $G = 20$
- 1.3 mas at $G = 21$

The proper motions uncertainties are

- 0.02 – 0.03 mas/yr for $G < 15$
- 0.07 mas/yr at $G = 17$
- 0.5 mas/yr at $G = 20$
- 1.4 mas/yr at $G = 21$

Radial velocities at *Gaia EDR3* hence contains *Gaia DR2* (Data release 2) median radial velocities for about 7.21 million stars with a mean G magnitude between ~ 4 and ~ 13 . The overall precision of the radial velocities at the bright end is of the order of $\sim 200 - 300$ m/s while at the faint end, the overall precision is ~ 1.2 km/s.]

Data Filtering and Completeness. According to *Gaia EDR3* data, we filtered stars with distances closer to 20 pc to the Sun ($\pi \geq 50$ mas). We obtained 2626 stars, including 677 stars with available radial velocity V_r (according to *Gaia DR2*). We selected stars with V_r relative error less than 20%.

For the Hyades OSC, we match the latest available catalog of the Hyades stars [13] with *Gaia EDR3* catalog.

Both field stars and Hyades stars samples are presented in Figures 1,2 in the projection on the Galaxy plane. Black dots represent the stars, color represent levels of equal density ($n_{levels} = 10$).

For the field stars, we can estimate the completeness of the data by considering the dependence of the number of stars on the distance to them. The completeness of the sample is sufficient until the moment when the number of stars begins to decrease. Thus, as we can see in Figure 3, the completeness of our stars sample is up to ~ 19 pc.

Integration Method. We integrated backward on 500 Myr field stars and Hyades stars during its motion in the Galaxy disk using *galpy*. The main assumption is the representation of the stars as a point.

In *galpy*, Galaxy is represented with Milky Way potential (MWPotential2014), described in [5]. This potential reproduces the Milky Way rotation curve and includes the disk, bulge, and spherical (halo) components of the Galaxy. The disk is given in the Miyamoto-Nagai expressions ([18]) and the spherically symmetric spatial distribution of the dark matter density in the halo by the Navarro-Frank-White profile ([19]).

To calculate the minimal distance d_{min} between each stars pair, we unloaded the galactocentric cartesian coordinates X, Y, Z and applied an algorithm to calculate the euclidian distance between each star pair. Minimal distance is a distance of the minimal approach between pair of stars during their motion in the Galaxy disk on a considered time interval. Then, for each pair we selected d_{min} and corresponding time t_{min} . The algorithm avoids repetition, thus, we get a complete statistical picture of the distances between all the stars we have chosen on the considered time interval.

Calculation Results. As a result of backward orbit integration, we listed minimal distances d_{min} and corresponding times t_{min} of the stars pairs.

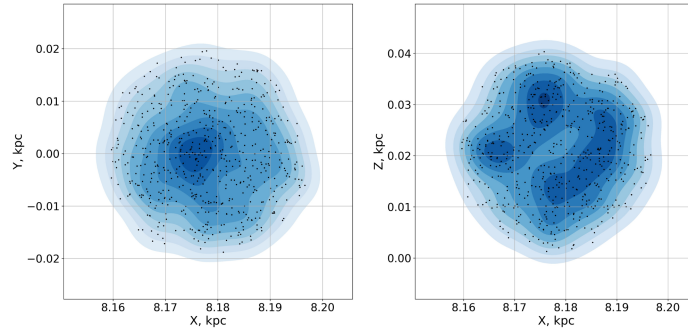


Fig. 1. Field stars sample according to *Gaia EDR3* in Galactocentric cartesian coordinate system. Directions of the coordinate axes: the X-axis is directed to the Galaxy center, the Y-axis is in the direction of the Galaxy disk rotation, and the Z-axis is to the North Pole of the Galaxy.

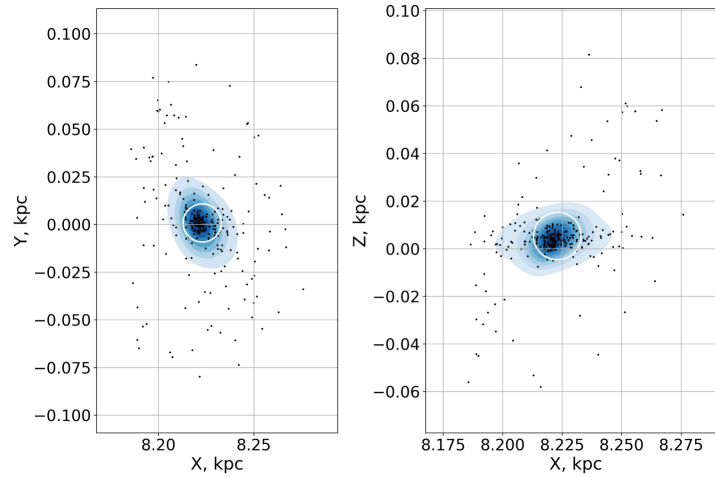


Fig. 2. Hyades OSC member stars sample according to *Gaia EDR3* in Galactocentric cartesian coordinate system. The white circle ($r = 10$ pc) shows the cluster core.

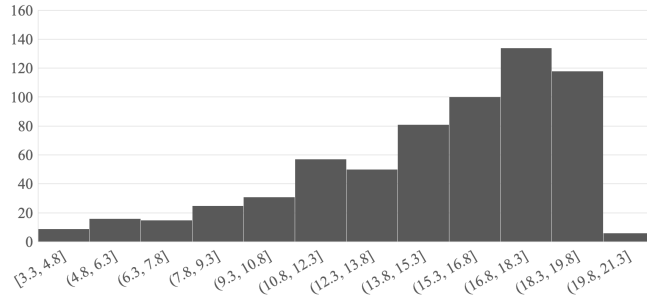


Fig. 3. Dependence of the number of field stars (ordinate or vertical axis) of our sample (see Fig. 1) on the distance to them (abscissa or horizontal axis, pc).

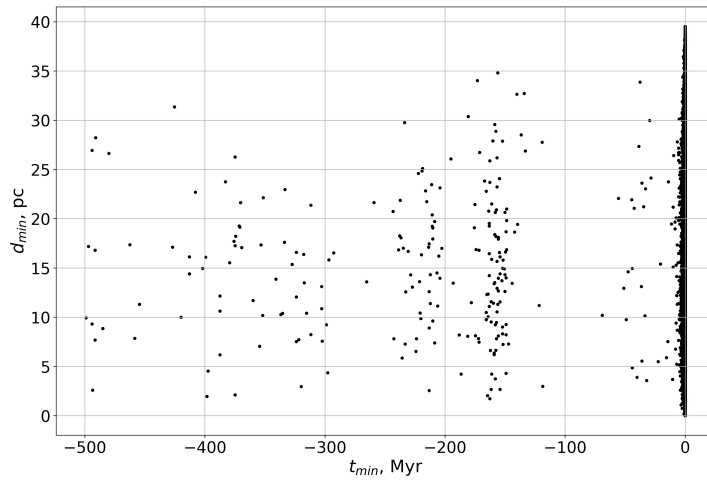


Fig. 4. The result of the integration of the field stars sample (see Fig. 1) The black dots show pairs of stars, the minimum distances between which were d_{min} at the time t_{min} on the considered time interval 500 Myr in the past.

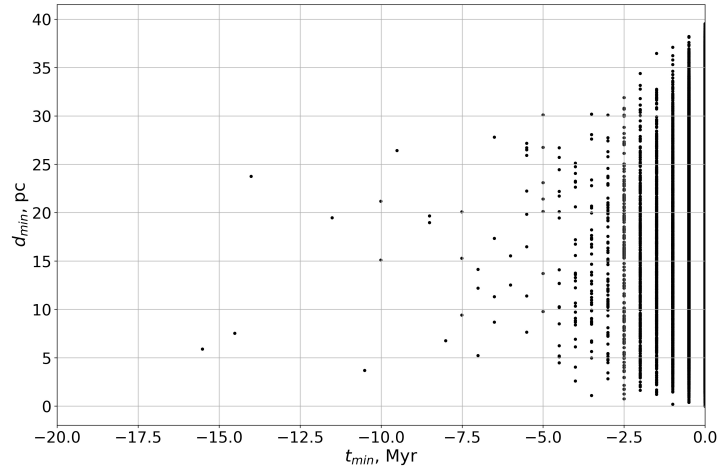


Fig. 5. The result of the integration of the fielded stars sample for the time interval up to -20 Myr.

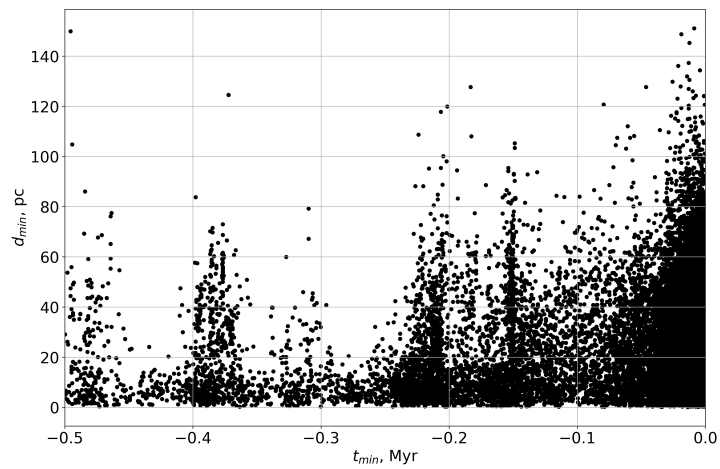


Fig. 6. The result of the integration of the Hyades star cluster stars sample (see Fig. 2). Here are clearly visible places of point concentration, or "resonances", arising due to differences in the orbits of stars from circular orbits.

3 Close Star Pairs

Now, we consider such pairs that approach close enough to affect the outer boundaries of the Oort clouds of each other. Results for field pairs and Hyades pairs with minimal distance less than 1 pc are shown in Figure 7. Table 2 contains list of the $d_{min}-t_{min}$ and ID according to *Gaia EDR3* for the field and Hyades stars (see Appendix A). Extremely close pairs ($d_{min} < 0.05$) in the Table 2 could be a binary stars, or an encountering pairs with accidentally unaccounted calculation error.

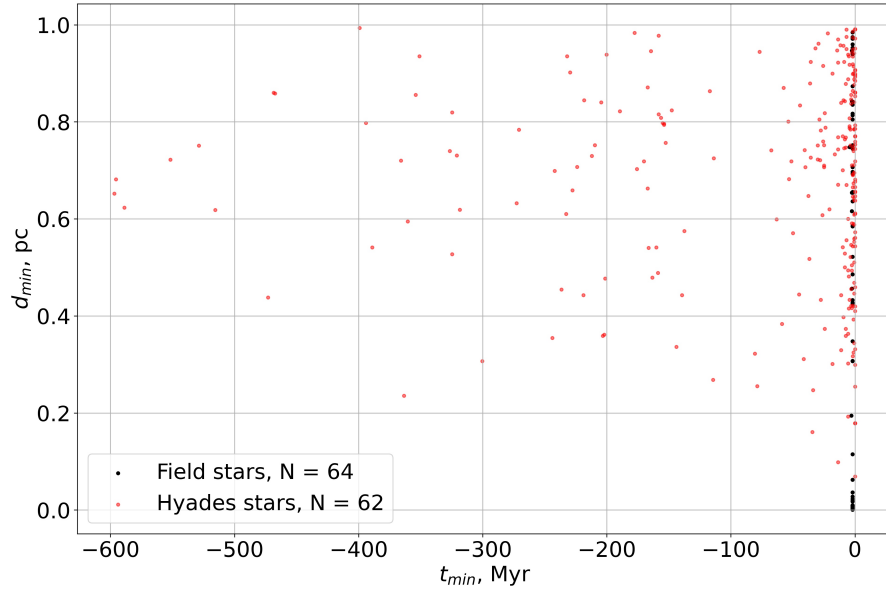


Fig. 7. The result of the integration of the Hyades star cluster stars sample (see Fig. 2).

Affecting of the Input Parameters Errors. The integration output depends not only on the orbit parameters but also on the Sun distance to the Galaxy center and its circular velocity R_0 and V_0 . R_0 is defined in dozens of publications, different authors received values in the range of 7.4 to 8.7 kpc. In [14] was investigated so-called "majority merging effect" consisting in choosing closer to previously published and expected values. It turned out that it is practically impossible to choose the most reliable value of R_0 . Changes in V_0 lead to the time shift: increasing V_0 will lead to an earlier approach and vice versa. We used $R_0 = 8.178$ kpc [8] and $V_0 = 232.8$ km s⁻¹ [16].

To estimate the uncertainties in determination d_{min} and t_{min} , we calculated d_{min} and t_{min} in extreme error values of the right ascension and declination (α ,

δ), proper motions (μ_α, μ_δ) , and radial velocity (V_r). As a result we obtained d_{min}^+, t_{min}^+ and d_{min}^-, t_{min}^- by integration with input values $\alpha \pm \sigma_\alpha, \delta \pm \sigma_\delta, \mu_\alpha \pm \sigma_{\mu_\alpha}, \mu_\delta \pm \sigma_{\mu_\delta}, V_r \pm \sigma_{V_r}$. Although it should be noted that *Gaia* errors of the astrometric parameters have cross-correlations, which we did not take into account here. For the stars in Figure 7 errors described below do not exceed 20%.

3.1 Estimation of the Interstellar Comets Number in the Galaxy

Obtained results allow us to estimate the number of events that can produce interstellar small bodies. The list of values for calculations is presented in Table 1. Columns contain time intervals we integrated for searching close pairs, number of stars in the sample, spatial size and volume of the sample, number of pairs for which we calculated the minimal distance, and number of close pairs that can produce the interstellar small bodies. Stars sample at time moment $t=0$ presented at Fig. 1 for field stars and 2 for the Hyades star cluster.

Table 1. Parameters of the stars samples.

	Field stars (Figure 1)	Hyades / core (Figure 2)
Number of stars	642	280 / 150
X, Y, Z (pc)	$36.9 \times 38.4 \times 39$	$90.3 \times 163.6 \times 139.5$
Volume (pc ³)	$5.5 \cdot 10^4$	$2.1 \cdot 10^6 / 0.8 \cdot 10^4$
Number of pairs	205,760	26,948
Number of pairs (<1 pc)	64	62

Now we could estimate the rate of producing the interstellar small bodies by field stars and by open clusters.

From the table, we see that the OSC produces 62 close pairs for 500 Myr, and the field stars produce 64 close pairs for the same period for a considered volume. There are 10^5 OSCs in the Galaxy, which means that the clusters replenish the ACP population of the Galaxy by 62×10^5 objects in 500 Myr, or 1.24×10^4 ACP in a 1 Myr.

The volume of the Galaxy V is the volume of a cylinder with a height of 2 kpc and a base area $S = 2\pi R$, where R is the radius of the Galaxy of 16 kpc. Thus, $V = 2 \times 2\pi \times 16 = 201$ kpc³. If for the volume calculated by us 5.5×10^{-5} kpc³ the productivity is 64 close pairs, then for the entire Galaxy it will be 2.35×10^8 in 500 Myr, or 47×10^4 ACP in a 1 Myr.

Next, we calculate the density of the ACP in the Galaxy. The age of the Galaxy is 1.35×10^{10} , thus, over the entire period of its existence were produced 0.67×10^{10} interstellar ACP. The ACP density is $\rho = \frac{0.67 \times 10^{10}}{201} = 3.3 \times 10^8$ ACP per 1 kpc³.

It should be noted, that close flyby may not cause noticeable disruption of the Oort cloud (see, for example, [15]).

Besides, note that our estimate does not take into account those stars that left the circumsolar neighborhood and could also approach both other stars and the Sun. Taking such encounters into account will increase the number of paired encounters and the number of free ACP objects, respectively.

4 Conclusions

The main results of the work are as follows.

- Using filters to restrict Big Data of the *Gaia EDR3* spacecraft, we composed samples of the field stars ($n = 642$) and the Hyades cluster stars ($n = 280$). Thus, only a small percentage of *Gaia* stars can still be used for our research. To accumulate the growing amount of data, it is possible to use the Russian Virtual Observatory.
- The integration of the motion of the stars around the Galaxy center in past epochs was carried out. Using the developed algorithm, we calculated the minimal distances d_{min} and corresponding time t_{min} of the star pairs of our sample (Fig. 4, 5, 6), and considered pairs that could provide interstellar small bodies (Fig. 7). Found pairs of stars approaching at a critical distance that may cause a loss of comets from their Oort clouds.
- We estimated the frequency of the interstellar small bodies production over the past 500 million years. Assuming that one close encounter delivers at least one ACP object to interstellar space, we obtained that the density of interstellar ACP is 3.3×10^8 ACP per 1 kpc^3 . Thus, about 10% of stars in the Galaxy may provide an interstellar ACP. This estimate is consistent with the observed data on the number of planetary systems in the Galaxy [11].

As part of this task, we encountered technical limitations specific to working with big data. First, the *Gaia* data contains terabytes of information, so we are forced to artificially limit the sample of stars under our study (in our case, by parallaxes, that is, by the distance from the Sun). Second, our computational capabilities are also limited, which prevents us from performing a pairwise search on a large amount of *Gaia* data. However, the *Gaia* data itself also has a number of limitations - even with an unlimited power reserve, we would face the problem of a lack of information in terms of radial velocities (astrometry of stars is much simpler and more accurate than spectral studies), as well as the limited observable part of the Galaxy. Nevertheless, even these problems can be partially solved using modern machine learning methods - the available sample of stars is enough to use the so-called "supervised learning" method, which would allow us to calculate statistics of stellar encounters across the entire disk. It is worth mentioning that machine learning is widely applied in astronomy, including open clusters studying (see, for example, the paper on searching for solar siblings [23], or on searching new open clusters in the Galaxy [12]).

Acknowledgments. This work presents results from the European Space Agency (ESA) space mission *Gaia*. *Gaia* data are being processed by the *Gaia* Data Processing and Analysis Consortium (DPAC). Funding for the DPAC is provided by national institutions, in particular the institutions participating in the *Gaia* MultiLateral Agreement (MLA). The *Gaia* mission website is <https://www.cosmos.esa.int/gaia>. The *Gaia* archive website is <https://archives.esac.esa.int/gaia>. The authors thank the reviewers for their helpful comments. Authors acknowledge the support of Ministry of Science and Higher Education of the Russian Federation under the grant 075-15-2020-780 (N13.1902.21.0039).

References

1. ESA *Gaia* EDR3 page, <https://www.cosmos.esa.int/web/gaia/earlydr3>
2. NASA exoplanets catalog, <https://exoplanets.nasa.gov/discovery/exoplanet-catalog/>
3. Bobylev, V.V., Bajkova, A.T.: Study of Close Stellar Encounters with the Solar System Based on Data from the Gaia EDR3 Catalogue. *Astronomy Letters* **47**(3), 180–187 (Mar 2021). <https://doi.org/10.1134/S1063773721020031>
4. Borisov, G.V., Shustov, B.M.: Discovery of the First Interstellar Comet and the Spatial Density of Interstellar Objects in the Solar Neighborhood. *Solar System Research* **55**(2), 124–131 (Mar 2021). <https://doi.org/10.1134/S0038094621020027>
5. Bovy, J.: galpy: A python Library for Galactic Dynamics. *The Astrophysical Journal* **216**(2), 29 (Feb 2015). <https://doi.org/10.1088/0067-0049/216/2/29>
6. Gaia Collaboration: VizieR Online Data Catalog: Gaia EDR3 (Gaia Collaboration, 2020). VizieR Online Data Catalog I/350 (Nov 2020)
7. Gaia Collaboration, Brown, A.G.A.e.a.: Gaia Early Data Release 3. Summary of the contents and survey properties. *Astronomy and Astrophysics* **649**, A1 (May 2021). <https://doi.org/10.1051/0004-6361/202039657>
8. Gravity Collaboration, Abuter, R., et. al: A geometric distance measurement to the Galactic center black hole with 0.3% uncertainty. *Astronomy and Astrophysics* **625**, L10 (May 2019). <https://doi.org/10.1051/0004-6361/201935656>
9. Johnson, S.A., Penny, M., Gaudi, B.S., Kerins, E., Rattenbury, N.J., Robin, A.C., Calchi Novati, S., Henderson, C.B.: Predictions of the Nancy Grace Roman Space Telescope Galactic Exoplanet Survey. II. Free-floating Planet Detection Rates. *The Astronomical Journal* **160**(3), 123 (Sep 2020). <https://doi.org/10.3847/1538-3881/aba75b>
10. Kiefer, F., Lecavelier des Etangs, A., Boissier, J., Vidal-Madjar, A., Beust, H., Lagrange, A.M., Hébrard, G., Ferlet, R.: Two families of exocomets in the β Pictoris system. *Nature* **514**(7523), 462–464 (Oct 2014). <https://doi.org/10.1038/nature13849>
11. Kunitomo, M., Matthews, J.M.: Searching the Entirety of Kepler Data. II. Occurrence Rate Estimates for FGK Stars. *The Astronomical Journal* **159**(6), 248 (Jun 2020). <https://doi.org/10.3847/1538-3881/ab88b0>
12. Leung, H.W., Bovy, J.: Deep learning of multi-element abundances from high-resolution spectroscopic data. *Monthly Notices of the Royal Astronomical Society* **483**(3), 3255–3277 (Mar 2019). <https://doi.org/10.1093/mnras/sty3217>
13. Lodieu, N., Smart, R.L., Perez-Garrido, A., Silvotti, R.: VizieR Online Data Catalog: A 3D view of the Hyades population (Lodieu+, 2019). VizieR Online Data Catalog J/A+A/623/A35 (Jan 2019)

14. Malkin, Z.M.: On the calculation of mean-weighted value in astronomy. *Astronomy Reports* **57**(11), 882–887 (Nov 2013). <https://doi.org/10.1134/S1063772913110048>
15. Mamajek, E.E., Barenfeld, S.A., Ivanov, V.D., Kniazev, A.Y., Väisänen, P., Beletsky, Y., Boffin, H.M.J.: The Closest Known Flyby of a Star to the Solar System. *The Astrophysical Journal* **800**(1), L17 (Feb 2015). <https://doi.org/10.1088/2041-8205/800/1/L17>
16. McMillan, P.J.: The mass distribution and gravitational potential of the Milky Way. *Monthly Notices of the Royal Astronomical Societys* **465**(1), 76–94 (Feb 2017). <https://doi.org/10.1093/mnras/stw2759>
17. Meingast, S., Alves, J.: Extended stellar systems in the solar neighborhood. I. The tidal tails of the Hyades. *Astronomy and Astrophysics* **621**, L3 (Jan 2019). <https://doi.org/10.1051/0004-6361/201834622>
18. Miyamoto, M., Nagai, R.: Three-dimensional models for the distribution of mass in galaxies. *Publications of the Astronomical Society of Japan* **27**, 533–543 (Jan 1975)
19. Navarro, J.F., Frenk, C.S., White, S.D.M.: Simulations of X-ray clusters. *Monthly Notices of the Royal Astronomical Societys* **275**(3), 720–740 (Aug 1995). <https://doi.org/10.1093/mnras/275.3.720>
20. Rickman, H.: Stellar Perturbations of Orbits of Long-period Comets and their Significance for Cometary Capture. *Bulletin of the Astronomical Institutes of Czechoslovakia* **27**, 92 (Jan 1976)
21. Torres, S., Cai, M.X., Brown, A.G.A., Portegies Zwart, S.: Galactic tide and local stellar perturbations on the Oort cloud: creation of interstellar comets. *Astronomy and Astrophysics* **629**, A139 (Sep 2019). <https://doi.org/10.1051/0004-6361/201935330>
22. Tutukov, A.V.: Stars and Planetary Systems. *Soviet Astronomy* **31**, 663 (Dec 1987)
23. Webb, J.J., Price-Jones, N., Bovy, J., Portegies Zwart, S., Hunt, J.A.S., Mackereth, J.T., Leung, H.W.: Searching for solar siblings in APOGEE and Gaia DR2 with N-body simulations. *Monthly Notices of the Royal Astronomical Societys* **494**(2), 2268–2279 (May 2020). <https://doi.org/10.1093/mnras/staa788>

A Table with d_{min} and t_{min} pf the close star pairs (see section 3)

Table 2: Parameters of the stars samples.

Type	Gaia EDR3 id1	Gaia EDR3 id2	d_{min} , pc	$t_{[min]}$, Myr
field	1872046609345556480	1872046574983497216	0.00055	0
field	1022456139210632064	1022456104850892928	0.00056	0
field	5559265690666327168	5559265690666326016	0.00179	0
field	5443051537858529792	5443051537858529920	0.00186	0
field	386653747925624576	386653851004022144	0.00271	0
field	732856080807636224	732857558276385664	0.00358	0
field	4955395178633330432	4955395178633330304	0.00424	0

Table 2: Parameters of the stars samples.

Type	Gaia EDR3 id1	Gaia EDR3 id2	d_{min} , pc	$t_{[min]}$, Myr
field	4986970575602213632	4986970575602213504	0.00459	0
field	1237090738916392832	1237090738916392704	0.00500	0
field	4519789321942643072	4519789081415296128	0.00539	0
field	1071194431653425280	1071195187567668480	0.00660	0
field	4911306239828325632	4911306239828325760	0.00708	0
field	461701979229013376	461701979233050624	0.00774	0
field	263916742385357056	263916708025623680	0.00779	0
field	3936909723803146368	3936909723803146496	0.00847	0
field	3057712188691831936	3057712223051571200	0.00884	0
field	43335880716390784	43335537119385216	0.00925	0
field	4364527594192166400	4364480521350598144	0.00939	0
field	3712538811193759744	3712538708114516736	0.00969	0
field	5291028284195365632	5291028181119851776	0.00984	0
field	3812355328621651328	3812355294262255104	0.01760	0
field	4722111590409480064	4722135642226902656	0.01881	0
field	3498481592531208576	3498481519515679872	0.02295	0
field	853819947756949120	853820948481913472	0.02763	0
field	5951165616611763456	5951165616635298816	0.03612	0
field	3394298532176344960	3400292798990117888	0.06225	0
field	3837746380705638656	3837697972130323456	0.11509	0
field	4038724053986441856	579567598501642368	0.19464	-1.0010
field	3060788519149063680	3057712188691831936	0.30701	0
field	3060788519149063680	3057712223051571200	0.30728	0
field	1472718211053416320	1472903753640492160	0.34775	0
field	1408029436569383296	1359938520253565952	0.42527	0
field	1408029509584967168	1359938520253565952	0.42762	0
field	1408029509583934464	1359938520253565952	0.43257	0
field	3478160727866058368	646255212109355136	0.45622	-0.5005
field	3478127463341507072	3478160727866058368	0.48556	0
field	974536192658255104	974887555341533440	0.52180	0
field	5866992641380992256	5895265380327966464	0.58470	0
field	4706564427272810752	4706630501049679744	0.58553	0
field	1408029509584967168	4548562265603840768	0.61610	-0.5005
field	1092545710514654464	1093918828739878528	0.63606	0
field	4866978844438656768	4678664766393829504	0.65386	-0.5005
field	2287506148856660992	2299942278201276288	0.65398	0
field	4093301474693288960	4079684229322231040	0.65537	0
field	522863309964987520	426641955043723520	0.69301	0
field	892215482207937152	893214796542513280	0.69675	0
field	5945941905576552064	5925209583053212800	0.70644	0
field	5698188160215537920	5602386058511578368	0.74452	0
field	2964001014514075520	2395413147718069504	0.74830	-2.5025

Table 2: Parameters of the stars samples.

Type	Gaia EDR3 id1	Gaia EDR3 id2	d_{min} , pc	$t_{[min]}$, Myr
field	4805806449875760384	4805866957374888448	0.75198	0
field	4025850731201819392	4034171629042489088	0.80494	0
field	543789661932658432	551050046451136256	0.81364	0
field	5412250540681250560	5425628298649940608	0.81697	0
field	4247023886053586304	4248817876711932416	0.83519	0
field	1062935140823485184	1050678712910407424	0.84161	0
field	704967037090946688	6029992663310612096	0.84248	-0.5005
field	4270814637616488064	4270446404294208000	0.87358	0
field	522863309964987520	512167948043650816	0.93959	0
field	3828238392559860992	1237090738916392832	0.94686	-0.5005
field	2929062902976882304	2927791352138805504	0.95268	0
field	436648129327098496	438829629114680704	0.95995	0
field	6508401923473282432	6508776375901968640	0.97118	0
field	6673000841376349696	6697578465310949376	0.97479	0
field	5042734468172061440	5038817840251308288	0.98441	0
hyades	3313653894061044224	3313662896313355008	0.178	0
hyades	146160558879786624	3410640887035452928	0.192	-5.6306
hyades	3314063908819076352	3314079508140198528	0.254	0
hyades	146677879098433152	146687018788948224	0.299	0
hyades	3312644885984344704	3312575685471393664	0.324	-1.2512
hyades	3312136499294830848	3312197934506930944	0.344	-0.6256
hyades	3312899491645515776	3312951748510907648	0.410	0
hyades	3313778207594395392	3313689422030650496	0.419	0
hyades	3314109916508904064	3313689422030650496	0.446	-0.6256
hyades	3313662896313355008	3313689422030650496	0.459	0
hyades	146160558879786624	3312602348628348032	0.488	-158.90
hyades	3295883999449691264	3305871825637254912	0.521	-3.7537
hyades	3314079508140198528	144534724778235392	0.541	-389.13
hyades	3314212068010812032	3314109916508904064	0.543	0
hyades	145373377272257664	144534724778235392	0.559	-0.6256
hyades	3313653894061044224	3313689422030650496	0.561	0
hyades	3405113740864365440	3405909374965722368	0.572	0
hyades	3387573300585597184	3387381646261643776	0.589	-1.2512
hyades	3304412601908736512	3412605297699792512	0.607	-26.276
hyades	3311024789960504576	3310702770492165120	0.610	0
hyades	3313662896313355008	3313778207594395392	0.611	0
hyades	3314109916508904064	3313778207594395392	0.637	0
hyades	3312951748510907648	3312842042162993536	0.643	-0.6256
hyades	3313689422030650496	3312951748510907648	0.646	0
hyades	50327297200978176	50298125783225088	0.654	0
hyades	3307645131734449408	3307844864893938304	0.656	0
hyades	3308127405023027328	3307992336891315968	0.665	0

Table 2: Parameters of the stars samples.

Type	Gaia EDR3 id1	Gaia EDR3 id2	d_{min} , pc	$t_{[min]}$, Myr
hyades	3312644885984344704	3312613000147191808	0.673	-1.2512
hyades	3312575685471393664	3312564037520033792	0.676	0
hyades	3312575685471393664	108421608959951488	0.681	-595.59
hyades	3312899491645515776	3313689422030650496	0.681	0
hyades	3312575685471393664	3312613000147191808	0.694	-0.6256
hyades	47541100375011968	47813504381625088	0.695	-0.6256
hyades	3313778207594395392	3312951748510907648	0.718	0
hyades	3312899491645515776	3312842042162993536	0.744	0
hyades	3307844864893938304	50298125783225088	0.756	-152.65
hyades	3312613000147191808	3312842042162993536	0.759	0
hyades	3313653894061044224	3313778207594395392	0.769	0
hyades	145325548516513280	49231668222673920	0.784	-0.6256
hyades	3314212068010812032	3314063908819076352	0.793	0
hyades	3406823245223942528	144377803854541184	0.794	-153.90
hyades	3311179340063437952	51383893515451392	0.796	-153.90
hyades	3405988677241799040	3405113740864365440	0.852	0
hyades	3313259169388356608	3312709379213017728	0.855	-3.1281
hyades	3314063908819076352	3314109916508904064	0.859	0
hyades	3404850790083594368	3405127244241184256	0.861	0
hyades	3311492803955469696	3310640648085373824	0.884	0
hyades	3314109916508904064	3313662896313355008	0.888	-0.6256
hyades	3310702770492165120	3311492803955469696	0.892	0
hyades	47804394753757056	48203487411427456	0.896	0
hyades	3312951748510907648	3312613000147191808	0.898	0
hyades	3312136499294830848	45142206521351552	0.899	-1.2512
hyades	3313778207594395392	3312899491645515776	0.905	0
hyades	3312564037520033792	3312842042162993536	0.907	0
hyades	3307645131734449408	3310640648085373824	0.914	-1.2512
hyades	149313099234711680	144534724778235392	0.923	-8.7587
hyades	3406943091991364608	3405113740864365440	0.923	-35.660
hyades	3312575685471393664	3312899491645515776	0.941	-0.6256
hyades	47813504381625088	47345009348203392	0.949	-1.8768
hyades	3314109916508904064	3312951748510907648	0.951	0
hyades	3313689422030650496	3312842042162993536	0.971	0
hyades	3312951748510907648	3314213025787054592	0.990	0